

Thaw subsidence analysis for multiple wells on a gravel island

MALCOLM A. GOODMAN

Enertech Engineering and Research Co., 2600 Southwest Freeway, Suite 300, Houston, Texas 77098, USA

F. JOSEPH FISCHER AND DAVID L. GARRETT

Shell Development Co., P.O. Box 1380, Houston, Texas 77001, USA

Sea-floor settlement, particularly differential settlement, is important for off-shore island design. For gravel islands, differential settlement at the sea-floor may result in movement of the island surface which could cause damage to surface facilities and/or require substantial amounts of make-up gravel for maintenance of island elevation. For steel gravity-type structures, differential settlement at the sea-floor could cause large stresses within the structure due to loss of foundation support. The magnitude and distribution of settlement beneath an island is dependent on thaw geometry which in turn is dependent on well arrangement on the island surface. This raises the following question: What well arrangement is best in order to meet the combined needs for island design, casing design, and operational purposes? To provide information useful to answering this question, two different well configurations have been analyzed, one with wells clustered within a circle in the centre of the island and the other with wells on two concentric circles near the periphery of the island. The intent is to consider one case of concentrated thaw beneath the island centre and another case of thaw distributed more evenly relative to the total surface area of the island.

L'affaissement du fond marin, surtout le tassement différentiel, est important dans la conception des îles artificielles offshore. Pour les îles de gravier, le tassement différentiel sur le fond marin peut provoquer un mouvement de la surface de l'île qui pourrait endommager les installations de surface ou nécessiter l'apport de quantités importantes de gravier pour le maintien de la hauteur de l'île. Pour les structures lourdes en acier, le tassement différentiel au fond marin pourrait créer des contraintes importantes par suite de la perte d'appui de la fondation. L'ampleur et la distribution du tassement sur l'île dépend de la géométrie des processus de dégel qui, à son tour dépend de la disposition des puits à la surface de l'île. La question suivante se pose alors: quelle disposition des puits est optimale pour satisfaire les besoins combinés de la conception des îles, des tubages et de l'exploitation? Afin d'obtenir des informations utiles pour répondre à cette question, deux configurations de puits différentes ont été analysées, l'une disposant les puits à l'intérieur d'un cercle tracé au centre de l'île et l'autre disposant les puits sur deux cercles concentriques près de la périphérie de l'île. On veut par le fait même étudier un cas de dégel accéléré sous le centre de l'île et un cas de dégel plus uniforme par rapport à la superficie totale de l'île.

Proc. 4th Can. Permafrost Conf. (1982)

[Ed. note: Data have not been converted to SI units.]

Introduction

Problems associated with drilling and production activities in off-shore arctic regions will likely be worse than those experienced on-shore. The presence of warm relict permafrost off-shore coupled with the probability of significant amounts of clay, not generally found on-shore, is the principal concern. Also the close proximity of numerous wells, necessitated by artificial island or platform geometries, will magnify the permafrost problems. It is felt that these problems can be overcome with appropriate well designs.

As a result of warm production fluids passing through permafrost, thaw is generated around wells and may coalesce depending on well spacing. For closely spaced multiple wells, extensive thaw will induce loads on the well casings and will cause subsidence at the sea-floor, even when the permafrost table is located a hundred feet, or more, below the mudline.

The multiple-well, thaw-subsidence analysis pre-

sented in this paper is applied to the Alaskan Beaufort Sea off-shore area and is performed with a finite element stress-analysis computer code. Thaw-subsidence loading mechanisms of pore pressure reduction and stiffness reduction upon thaw are incorporated in the model. The effects of sea-floor pressure due to weight of a gravel island in 20 ft of water are also considered. Results are presented for displacements, strains, and stresses beneath the island, in the casing, and in the surrounding soil.

Thaw Subsidence Model

Four loading mechanisms contribute to permafrost thaw-subsidence (Goodman, 1977):

- (i) Excess ice melting;
- (ii) Thaw-consolidation due to expulsion of pore water (Morgenstern and Nixon 1971; Nixon and Morgenstern 1973);
- (iii) Pore pressure reduction; and
- (iv) Stiffness reduction.

The first two mechanisms are associated with ice-rich soils and, therefore, are applicable to surface soils where excess ice is commonly found. In sea-floor soils beneath the Beaufort Sea, excess ice has not been encountered. On the contrary, the upper clay-silt layer in the off-shore Prudhoe Bay region is generally over-consolidated with low water content (Sellmann and Chamberlain 1979). The third and fourth mechanisms are dominant in deep permafrost and both are employed in this study.

Pore Pressure Reduction

Pore pressure reduction is the basis for the Prudhoe Bay model developed by ARCO/Exxon (Mitchell 1977; Mitchell and Goodman 1978). In soils, as pore ice melts, the volume contraction of approximately ten per cent due to the phase change is accompanied by a decrease in pore pressure, i.e., unless fluid is supplied to the thawed soil to offset the volume change upon thaw, the pore pressure must decrease. This pore pressure reduction is supported by measured data from the ARCO/Exxon thaw-subsidence field test (Mitchell 1977).

For modelling purposes (Mitchell and Goodman 1978), the permafrost pore pressure before thaw is taken as the ice hydrostatic pressure, and the pore pressure after thaw is assumed to be zero (Mitchell and Goodman 1978). Hence, the pore pressure reduction is defined by

$$[1] \quad \Delta p = \rho_i g Z,$$

where ρ_i is the ice density. Based on field data the pore pressure does not decline completely to zero, but to some value less than about 200 psi. With the assumption of zero final pore pressure, Δp is maximum and this is conservative for subsidence predictions.

As pore pressure decreases, the soil matrix compacts (Figure 1). The pore pressure change acts across the thawed-frozen interfaces, squeezing the thaw

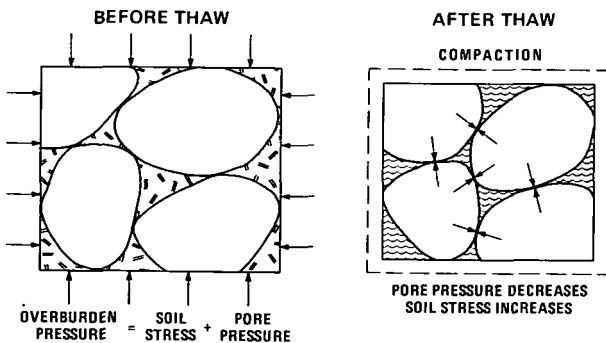


FIGURE 1. Permafrost compaction due to pore pressure reduction upon thaw.

front inward and the permafrost base upward (Figure 2). Similarly, in off-shore permafrost, the permafrost table will be squeezed downward.

In addition to the boundary pressure Δp at the thawed-frozen interface, the change in pore pressure also creates a body force loading within the thawed zone (see Figure 2). This body force is due to the loss in vertical support or buoyancy that was provided by the pore ice, causing the soil to compact vertically, and is defined as the gradient of Δp ,

$$[2] \quad \frac{d}{dZ} \Delta p = \rho_i g.$$

For $\rho_i g = 0.4$ psi/ft, the body force is 58 lb/ft³, which gives an apparent increase in weight of nearly 50 per cent for a soil with a density of 130 lb/ft³.

Stiffness Reduction

Although documented in the literature (Goodman 1977; Mitchell and Goodman 1978), stiffness reduction as a thaw-subsidence loading mechanism was not used in the Prudhoe Bay model. Stiffness reduction is associated with the difference in elastic properties between frozen and thawed soil, frozen soil having a higher modulus (Goodman 1975). Since the soil becomes weaker upon thaw, the overburden loads will cause the soil to compact, not only vertically, but also laterally. The lateral overburden pressure will squeeze the thaw front inward, in addition to the lateral squeeze due to pore pressure reduction.

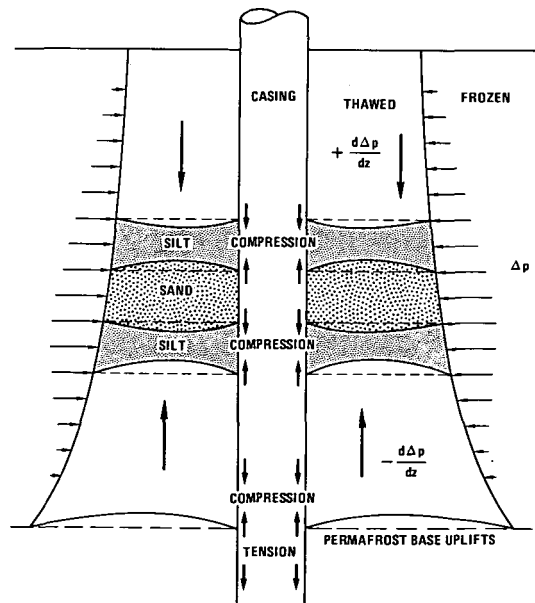


FIGURE 2. Pore pressure reduction loading mechanism.

The body force due to stiffness reduction is related to the change ΔE in elastic modulus and has the mathematical form

$$[3] \quad \frac{d}{dZ} \left[\frac{\Delta E}{E} \sigma \right] = - \frac{\Delta E}{E} (\rho - \rho_i) g,$$

where σ is the vertical effective overburden stress before thaw. Note that the body force due to stiffness reduction is generated because of the presence of initial stress σ . Without an initial stress, a change in stiffness alone would not cause thawed permafrost to deform.

For the values of E (Goodman 1975), it follows that $\Delta E/E = 0.354$. With $\rho g = 130 \text{ lb/ft}^3$ and $\rho_i g = 58 \text{ lb/ft}^3$, then the value determined from the above expression is 25.5 lb/ft^3 , which is roughly half that due to pore pressure reduction. But the two effects are additive and, hence, the total apparent increase in weight is 83.5 lb/ft^3 .

Gravel Island and Well Configurations

Two specific well arrangements have been analyzed for thaw-subsideance effects: first, a central casing cluster and, secondly, a system of annular casing rings. For the central cluster, 60 wells are grouped within a 100-foot diameter region centred on the gravel island (Figure 3). The 100-foot cluster is assumed to consist of a single composite material for

the purpose of analysis. This assumption is sufficient for prediction of soil stresses and displacements outside the cluster and is conservative from a casing strain stand-point since the modulus of the casing-soil composite is less than the casing steel.

An alternative 60-well layout for the gravel island has two annular rings of casings, one ring centred at a radius of 165 ft, and the other at 225 ft (Figure 4). The rings are treated as composite soil-casing systems with each ring ten feet thick in the radial direction and containing 30 wells distributed evenly around the ring in the hoop direction.

A gravel island in 20 ft of water generates sea-floor pressures that contribute to soil deformation. In addition, the island weight creates an initial stress before thaw that affects the stiffness reduction loads after thaw. For this study, the gravel island has a working-surface diameter of 500 ft, a sea-floor diameter of 800 ft, and a freeboard of 20 ft. Beneath the working surface, sea-floor pressures are 33.7 psi which includes equipment weight as well as gravel weight.

Permafrost Description and Thaw Geometry

For the off-shore Alaskan region of interest, the permafrost base is assumed to be 1800 ft below the sea-floor. The top of the permafrost is 125 ft below the sea-floor. The thaw radius due to oil production from the central casing cluster (see Figure 3), has

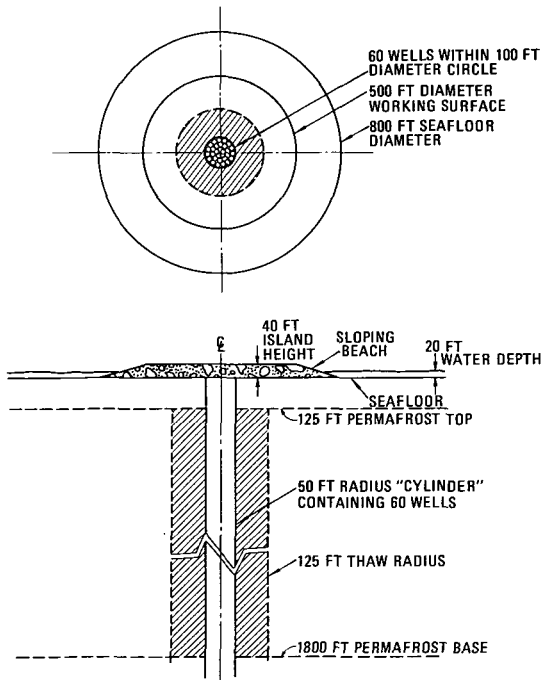


FIGURE 3. Central cluster well arrangement.

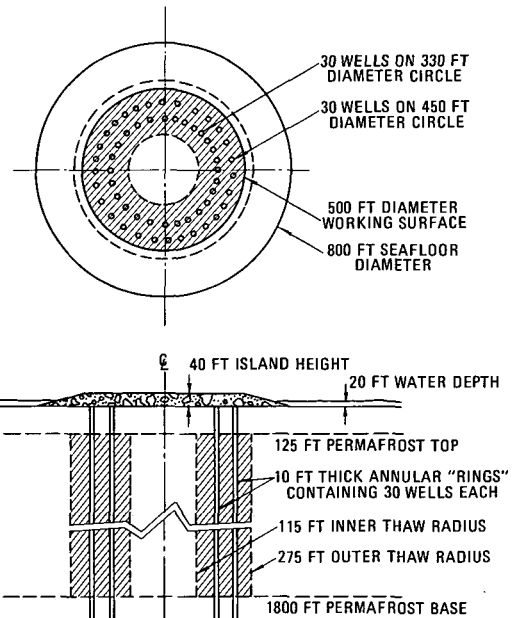


FIGURE 4. Annular ring well arrangement.

been estimated to be 125 ft, giving 75 ft of thaw beyond the casing cluster. For the annular rings of casing (see Figure 4), thaw is assumed to be completely coalesced between wells and between casing rings, and extends 50 ft inward from the inner ring and 50 ft outward from the outer ring. This thaw geometry contains an inner frozen core 230 ft in diameter.

Except for the clay-silt layer in the upper 25 ft, the soil is assumed to be sand. Young's modulus for the clay-silt layer is taken to be 2500 psi. The Young's modulus, E , for the unfrozen soil above the permafrost table is assumed to vary linearly with depth, Z ,

$$E = 41 Z \text{ psi}, \quad 25 < Z < 125 \text{ ft.}$$

Within and below the permafrost, the modulus is assumed to vary with the square root of depth (Goodman 1975):

$$E_u = 1150\sqrt{Z} \text{ psi}, \quad 125 < Z$$

$$E_f = 1780\sqrt{Z} \text{ psi}, \quad 125 < Z < 1800 \text{ ft,}$$

where E_f is for frozen soil, and E_u is for unfrozen soil and thawed permafrost. Poisson ratio is taken to be 0.33.

Displacements and Stresses due to Gravel Island

Placement of the gravel island will induce loads and deformations on the sea-floor and subsurface soils. Vertical displacement profiles for four selected depths (Figure 5) show that downward movement is greatest beneath the island centre and decreases toward the island edge, generating differential settlement. Maximum displacement of the sea-floor ($Z = 0$) is 1.1 ft at $r = 0$, diminishing to less than 0.2 ft at $r = 400$ ft. However, at $r = 250$ ft, which is directly beneath the edge of the island working surface, displacement is 0.9 ft and, hence, the differential settlement across the working surface is only 0.2 ft. It should be noted that this differential settlement is at the sea-floor and that the associated differential settlement of the actual working surface should be somewhat less.

Island placement effects are damped out with increasing depth below the sea-floor. At a depth of 125 ft, vertical displacement is less than 0.45 ft compared to 1.1 ft at the sea-floor. This decreases to 0.1 ft at a depth of 600 ft.

Incremental vertical stresses due to island placement are presented (Figure 6). Stresses are greatest

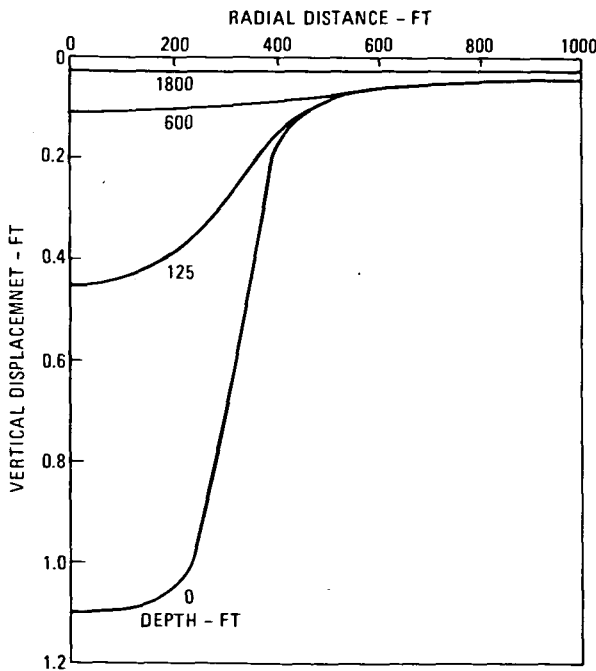


FIGURE 5. Vertical displacements due to ground island placement.

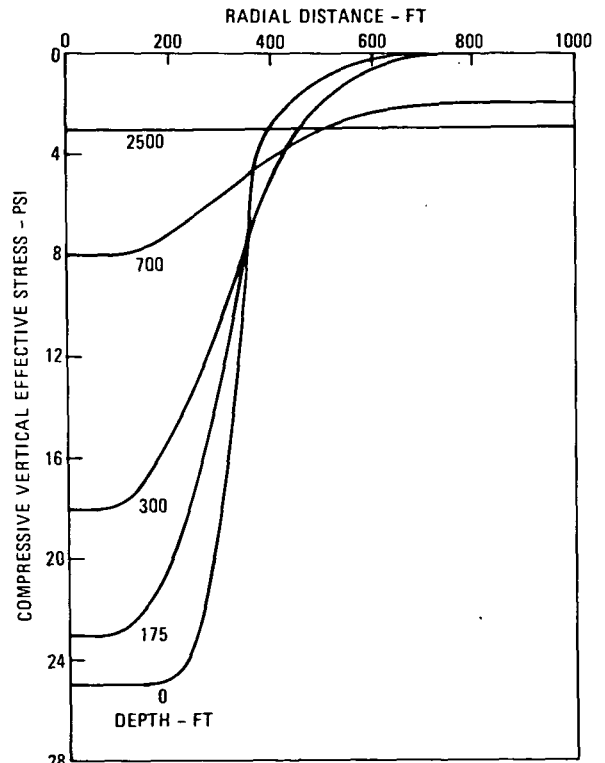


FIGURE 6. Instrumental vertical stress due to island placement.

along the sea-floor beneath the island, but vanish rapidly as the island edge is approached and also diminish with depth below the sea-floor. The stress profiles cross each other at the island edge, indicating that arching behavior transmits the island forces to the deeper soils beyond the island ($r > 400$ ft). Maximum values of the incremental stresses are 25 psi for the vertical effective stress and 13 psi for the horizontal effective stress. Total stresses due to overburden weight and island placement indicate that the sea-floor soils may yield beneath the outer edge of the island.

Vertical Displacements due to Thaw

Central Casings: Vertical displacements for the central casing problem are plotted against radius (Figure 7) for five different depths. Downward movement is taken as positive and upward movement is negative. As expected, the permafrost base and table

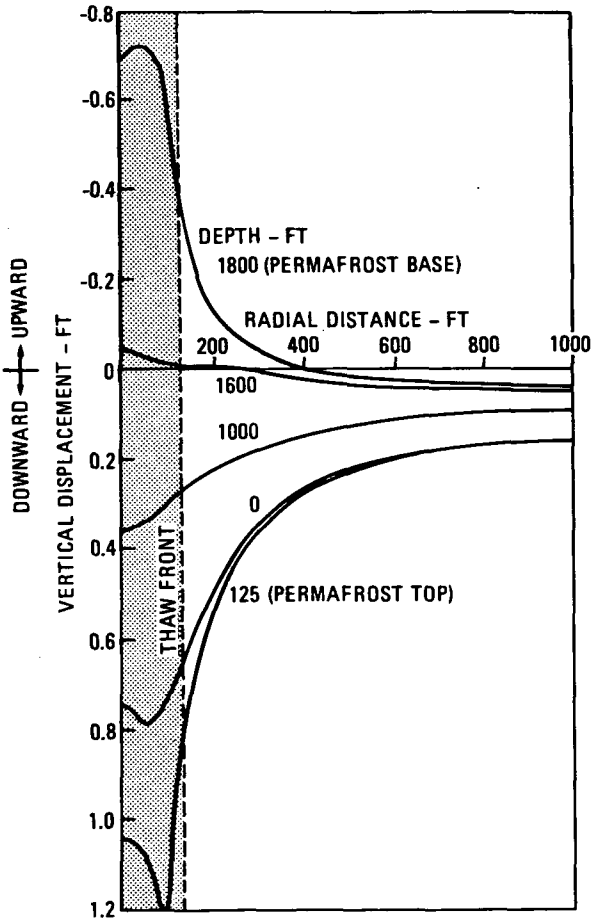


FIGURE 7. Vertical displacement due to thaw around central casing cluster.

move inward to the thaw zone due to pore pressure reduction and stiffness reduction across each interface, i.e., the base at the depth of 1800 ft moves upward and the table at 125 ft moves downward.

The sea-floor $Z = 0$ moves with the permafrost top, but the downward movement at the sea-floor is less. Note that the displacements do not reach a maximum at $r = 0$, but at some radius between the casing and the thaw front. This is due to the increased shear resistance from the casing. Along the sea-floor, displacements are 0.75 ft at the centre of the island, reaching a maximum of 0.80 ft at $r = 50$ ft and decreasing to 0.40 ft at the edge of the working surface at $r = 250$ ft.

Vertical movement at all depths diminishes with increasing radial distance from the thaw front. Beyond $r = 400$ ft, there is general downward movement at all depths, even at the base. At $r = 1000$ ft, the sea-floor moves down 0.16 ft and the base moves down 0.04 ft.

Total vertical movement due to island placement and thaw (Figure 8) represents the sum of values from

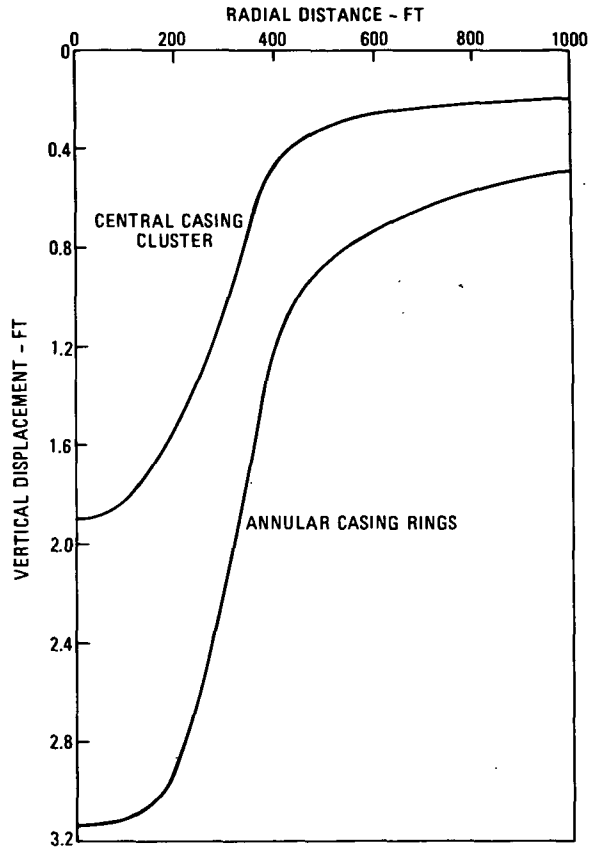


FIGURE 8. Total sea-floor displacement due to island placement plus thaw.

Figures 5 and 7. Maximum sea-floor displacement is 1.90 ft for the central casing system, decreasing to 1.35 ft at $r = 250$ ft. Differential sea-floor settlement is, therefore, equal to 0.55 feet across the extent of the working surface.

Annular Casing Rings: Vertical movement due to thaw around annular casings (Figure 9) is more than twice that in Figure 7 for the central cluster. The dip within the thaw zone is also more pronounced because of the added resistance of the interior frozen core. Total sea-floor movement due to island placement and thaw for the annular casings (see Figure 8) shows that maximum vertical displacement is 3.10 ft near the island centre and decreases to 2.55 ft at $r = 250$ ft. Although total movement for the annular casings is significantly greater due to increased thaw beneath the island (outer thaw radius is beyond the working surface), differential settlement at the sea-floor across the working surface is 0.55 ft which is the same as that for the central cluster.

Radial Displacements due to Thaw

Horizontal (radial) displacement of the thaw front is of interest qualitatively because soil reactions and

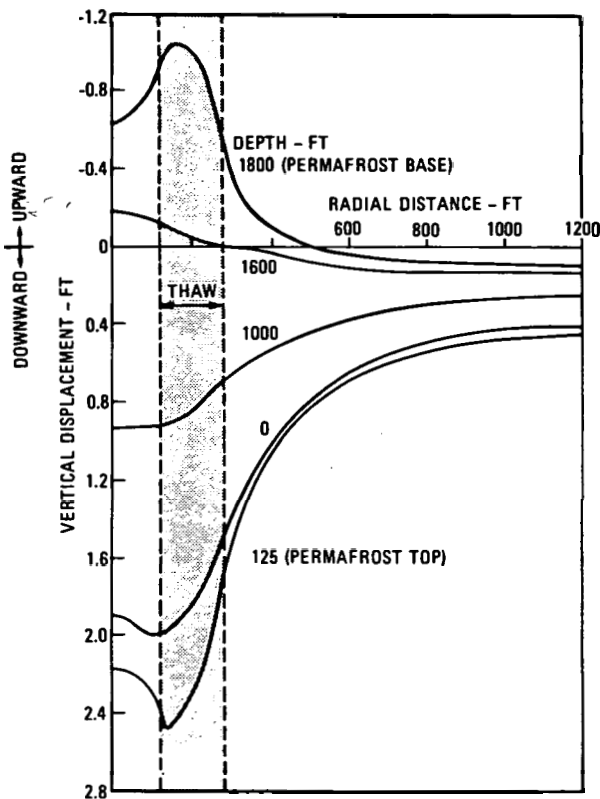


FIGURE 9. Vertical displacement due to thaw around annular casing rings.

casing strains are governed to a large extent by the inward movement of the thaw front. Inward radial squeeze can result in significant vertical stresses and strains via the Poisson ratio of the soil. In the ARCO/Exxon thaw test (Mitchell and Goodman 1978), the horizontal thaw front movement together with lithology layering accounted for the alternating tensile - compressive strains measured in the casing (see Figure 2).

Central Casing: Radial displacement profiles with depth are presented in Figure 10. Greatest horizontal displacement occurs at the thaw front ($r = 125$ ft) and increases with depth because of the greater pore pressure reduction and stiffness reduction in the deeper soils. The maximum (Figure 10) does not occur at the base, but above the base at a depth of 1500 ft. Lateral motion at the base is resisted by the soil beneath the base.

The response in the sea-floor soils down to a depth of 300 ft exhibits complex behaviour (Figure 10). As the permafrost top moves downward, the thawed soils bulge outward, tending to counteract the inward squeeze due to pore pressure and stiffness reduction. This accounts for the hump in the profile just below the permafrost table. In addition, the free surface at the sea-floor and the softer soils above the table do not offer much resistance to the inward movement

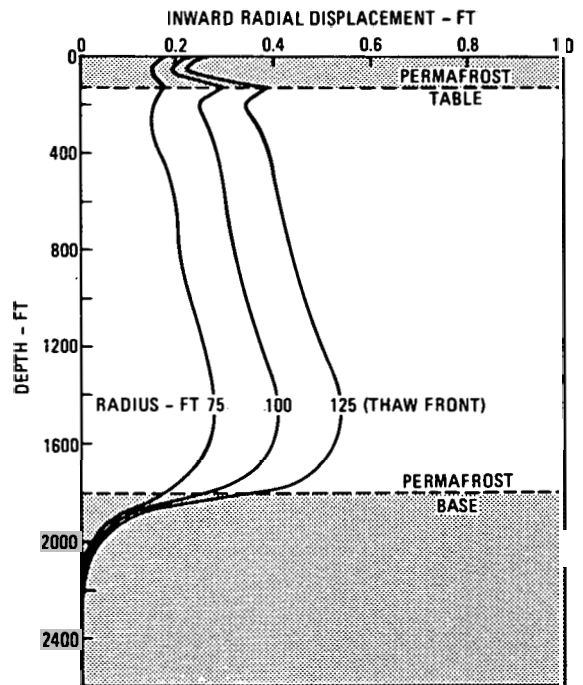


FIGURE 10. Radial displacement due to thaw around central casing cluster.

at the permafrost top, generating the peak at $Z = 125$ ft.

The displacement profiles above the table also show a hump (see Figure 10). In this region, the inward displacement decreases as expected for the unthawed soil, but the lateral stretching of the free surface as it is pulled downward reverses the trend.

Annular Casing Rings: Radial displacements occur with depth and radius, respectively. In Figure 11, the three profiles represent the inner and outer thaw fronts and the mid point between the two casing rings. Both thaw fronts are squeezed into the thaw zone, the outer front exhibiting positive (inward) movement and the inner front exhibiting negative (outward) movement. The profile of the outer front in Figure 11 is similar to the distributions in Figure 10, but the hump below the permafrost table is more pronounced due to the effect from the inner thaw front. Note that the inward motion of the sea-floor soils associated with the downward movement of the permafrost top dominates the behaviour in the upper regions, even at $r = 115$ ft.

The radial distributions (Figure 12) show the characteristic peaks at the inner and outer thaw fronts. Displacement gradients in the radial direction are steep, rising and falling sharply within and outside the thaw zone. At the 1400-foot depth, magnitude of the radial displacement reaches 0.9 ft., which is greater than the vertical displacement at this depth (see Figure 9).

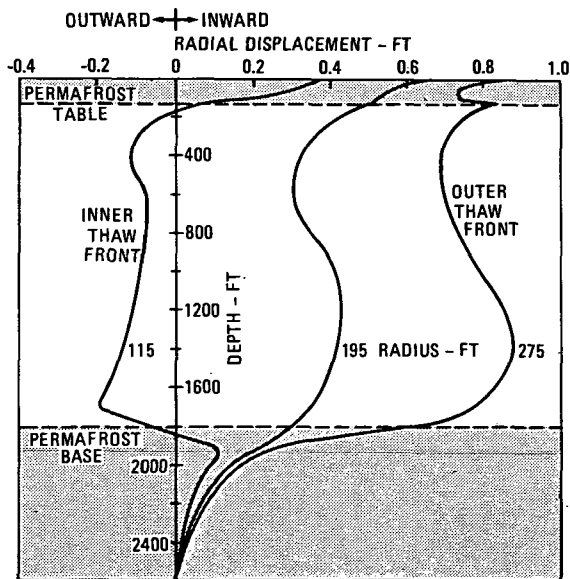


FIGURE 11. Radial displacement due to thaw around annular casing rings.

Soil Stresses due to Thaw

Stresses are important for yield assessment. Results for the central cluster are presented to demonstrate the interaction between thawed and frozen zones.

Vertical stresses due to thaw are plotted *versus* radius (Figure 13) for depths above and below the permafrost table, and above and below the permafrost base. Stresses within the permafrost are compressive and stresses outside are tensile. Magnitudes decrease rapidly with radius, becoming nearly zero at $r = 300$ ft. Maximum values for all depths occur at $r = 0$, except above the permafrost top where the maximum tension occurs away from the centre because of the free surface effect at the sea-floor.

In the radial stress distributions (Figure 14) within the thaw zone, radial stresses are compressive due to the inward movement. Beyond the thaw front, stresses are tensile with maximum tension occurring just above the base.

A key observation here is that both the radial and vertical stresses within the thaw zone increase compressively by approximately the same magnitude, indicating that the shear stresses in the thaw zone remain nearly constant while the normal stresses increase. This behaviour tends to stabilize the soil and prevent yielding. On the other hand, in the permafrost outside the thaw zone, the incremental radial stress becomes tensile while the vertical stress increases in compression. This causes the shear stress to

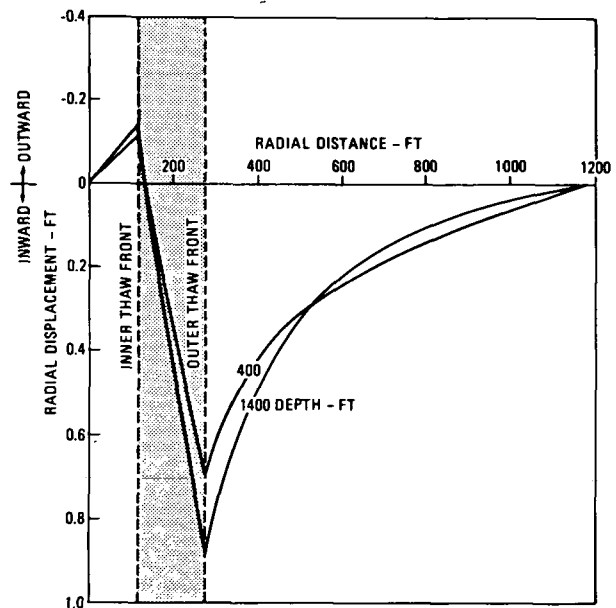


FIGURE 12. Radial variation of lateral displacements due to thaw around annular casing rings.

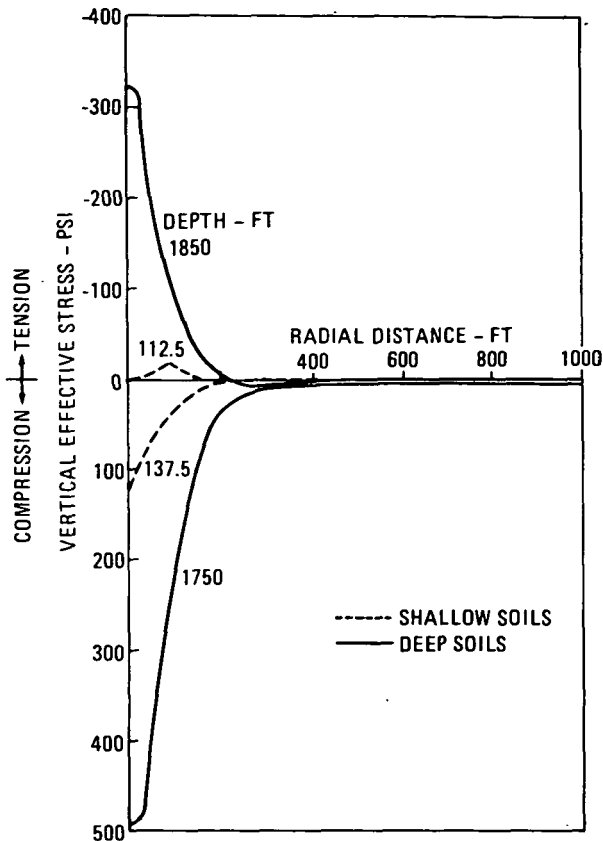


FIGURE 13. Incremental vertical stresses due to thaw around central casing cluster.

increase, tending to destabilize the soil with regard to yield.

From these results and interpretations, it follows that the thawed permafrost behaves differently than intuition suggests. Rather than becoming softer and slumping as one would expect, the thawed soil becomes more stable due to the inward squeeze.

Composite Casing Strain

Average strains have been determined for the casing-cement-soil system. These strains are conservative in the sense that the actual strains in the casings are less, but are not worst-case strains because the lithology is not layered. The Prudhoe Bay model (Mitchell and Goodman 1978) has shown that maximum strains for casing design purposes are generated when stiff layers lie adjacent to relatively soft layers. In this study, layering has not been considered.

The aim of this work is to evaluate the effect on casing strains of well arrangement (cluster *versus* annular rings) and of large coalesced thaw from multiple wells. In contrast, Prudhoe Bay results are for single wells only.

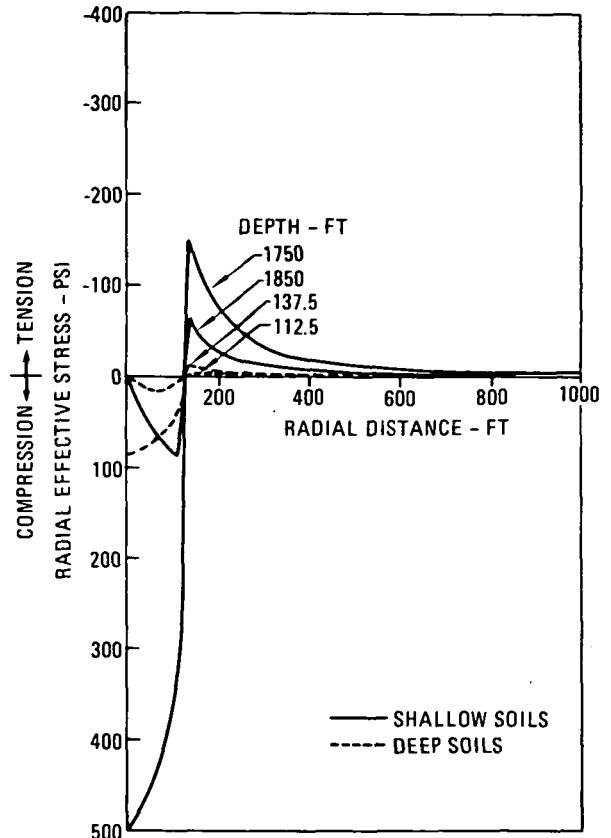


FIGURE 14. Incremental radial stress due to thaw around central casing cluster.

The predicted results for both the central cluster and annular ring systems are given (Figure 15). For the annular rings, the inner casing ring experiences greater strains than the outer ring and, hence, only the values for the inner ring are presented.

The compression peak above the base and tension peak below the base are characteristic of the uplift at the permafrost base. Similarly, the compression below the permafrost table and tension above are indicative of the downward movement of the permafrost top. The hump at the 500-foot depth is due to slumping of the softer soils above this depth.

In Figure 15, the strains above the permafrost table should be interpreted with caution because casing resistance in this zone has been neglected in the model.

Three important conclusions can be drawn from Figure 15. First, the composite casing strains for the annular ring arrangement are greater than for the central cluster. This is expected because of the larger thaw and lower composite moduli.

The second conclusion is that the maximum values of both the tensile and compressive strains at the

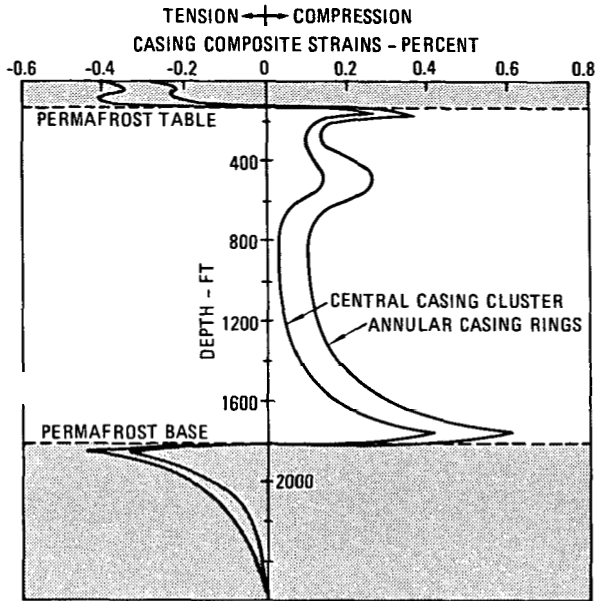


FIGURE 15. Casing composite strains due to thaw.

base, 0.45 and 0.61 per cent, respectively, are significantly greater than the predicted values (without layering) for single wells at Prudhoe Bay (Mitchell and Goodman 1978). In fact, the values in Figure 15 are nearly equal to the maximum expected values (due to worst-case layering) of 0.5 and 0.7 per cent used for single well casing design at Prudhoe Bay. This suggests that layering, which increases the casing strains at Prudhoe Bay by more than a factor of four, may increase the strains in Figure 15 to the point of exceeding the casing strain limit. However, for a soil volume change greater than nine per cent of the porosity, the soil is again saturated and the compaction process stops. The primary volume change has been computed to be due to inward radial motion of the thaw front. Thus, vertical strains are likely to be significantly less than nine per cent of the porosity. For 13³/₈-inch, 72-lb, N-80 buttress casing, the tensile and compressive strain limits are 3.4 and 2.3 per cent, respectively. If the strain limit is exceeded, then the composite modulus approach used in this study would have to be abandoned in favour of a more-detailed analysis of the casing to account for the well spacing in the horizontal plane.

The third conclusion involves the peak strain at the permafrost top. This behaviour does not occur in on-shore wells where permafrost begins at the surface. The significance of this peak is that it occurs relatively close to the sea-floor and, hence, will affect large-diameter conductor casing or intermediate permafrost casing that penetrates the permafrost table.

Strain limits of the larger casings are typically less than the 13³/₈-inch casing used at Prudhoe Bay. Special casing design considerations may be required for this upper zone. It should be noted, however, that the shear capacity of the near surface soils may be too low to impart this strain to the casing.

Conclusions

1. Displacements, stresses, and strains due to thaw are generally greater for the annular casing ring system compared to the central cluster system.

2. Maximum vertical sea-floor displacement due to island weight and thaw occurs beneath the island centre and is 1.9 ft for the central casing cluster and 3.1 ft for the annular rings. However, the differential displacements across the extent of the island working surface from the centre to the edge is the same (0.55 ft) for both well arrangements.

3. Casing strains are highest in the inner casing ring of the annular system, compared to the outer ring or to the central cluster. Maximum strains occur near the permafrost base and are 0.45 per cent tensile and 0.61 per cent compressive. Lithology layering can potentially increase these values. But the computed strains in the present model are average soil-casing composite strains which are greater than the actual strain in the casing. To analyze actual casing strains, a more complex and detailed approach that accounts for well spacing in the horizontal plane is required.

4. Peak tensile and compressive strains of 0.4 per cent occur at the permafrost table. Selection of conductor casing or intermediate permafrost casing passing through the permafrost table will need to consider these strains.

5. Maximum, vertical, soil effective stress due to island placement (in 20 ft of water) is 25 psi and maximum, radial, effective stress is 13 psi. The stresses at the sea-floor beneath the island edge indicate that the soil in this region may yield.

6. Permafrost thaw may generate further yield in the formation soils beneath the island, but the yielding is restricted to the region beneath and beyond the sloping edge of the island and occurs only in the upper layer.

7. Stresses within the permafrost interval are of interest because of the soil yield which is a natural mechanism for casing strain relief. Within the thaw zone, vertical and radial stresses both increase compressively, whereas outside the thaw zone, the vertical stress increases compressively but the radial stress decreases. This stress behaviour causes the thawed soil to become more stable with less tendency for yield, but generates high shear in the frozen soil just

outside the thaw front. For both the central cluster and the annular casing rings, yield in the frozen soil may occur along the entire permafrost section and, particularly, near the permafrost base where the highest casing strains are predicted. The model used for this study did not include yield behaviour, but simply noted which regions reached yield conditions. The results indicate that yield is significant and should be included in future studies.

Acknowledgement

The authors thank Shell Oil Company for support of this work and for permission to publish this paper.

References

- GOODMAN, M.A. 1975. Mechanical properties of simulated deep permafrost. *J. Eng. Ind., Trans. ASME*, vol. 97, Series B, No. 2, May, pp. 417-425.
- . 1977. Loading mechanisms in thawed permafrost around Arctic wells. *J. Pressure Vessel Technol., Trans. ASME*, vol. 99(4), November, pp. 641-645.
- MITCHELL, R.F. 1977. A mechanical model for permafrost thaw subsidence. *J. Pressure Vessel Technol., Trans. ASME*, vol. 99(1), February, pp. 183-186.
- MITCHELL, R.F. AND GOODMAN, M.A. 1978. Permafrost thaw-subsideance casing design. *J. Pet. Technol.*, vol. 30, March, pp. 455-460.
- MORGENSTERN, N.R. AND NIXON, J.F. 1971. One-dimensional consolidation of thawing soils. *Can. Geotech. J.*, vol. 8(4), pp. 558-565.
- NIXON, J.F. AND MORGENSTERN, N.R. 1973. Practical extensions to a theory of consolidation for thawing soils. *In: Proc. 2nd Int. Conf. Permafrost, Yakutsk, USSR, North Amer. Contrib., US Natl. Acad. Sci.*, pp. 369-376.
- SELLMANN, P.V. AND CHAMBERLAIN, E.J. 1979. Permafrost beneath the Beaufort Sea near Prudhoe Bay, Alaska. *In: Proc. Offshore Technol. Conf., Houston, Texas*, pp. 1481-1493.